Plasmonic Response of Bent Silver Nanowires for Nanophotonic Subwavelength Waveguiding

David Rossouw and Gianluigi A. Botton*

Department of Materials Science and Engineering, McMaster University, 1280 Main Street West, Hamilton, Ontario L8S 4L7, Canada

(Received 21 February 2012; published 6 February 2013)

We have imaged, with electron energy loss spectroscopy, the plasmonic response of straight and bent silver nanowires for their potential use in nanophotonic circuits. The guided surface plasmon polaritons appear unaffected by the presence of sharp kinks and corners in the nanowires studied, shown by direct imaging of excited Fabry-Perot-type resonances. Nanoscale detection is extended down to 0.17 eV, enabling detailed measurements of the spatial extent and dispersion of guided surface plasmon polaritons at low wave numbers. The experimental measurements are in excellent agreement with calculations, and the results are relevant in the design of integrated nanophotonic circuits and devices.

DOI: 10.1103/PhysRevLett.110.066801 PACS numbers: 73.20.Mf, 68.37.−d

Nanoscale photonic circuits based on surface plasmons are a promising alternative to replace electronic circuits in microprocessors and other computer chips, combining faster operating speeds and reduced power consumption in ultracompact architectures [1]. The miniaturization of photonic circuits down to the nanoscale for the fabrication of highly integrated nanophotonic circuits and devices requires electromagnetic energy to be manipulated on a subwavelength scale and guided in geometries containing sharp corners [2]. Noble metal nanowires support guided surface plasmon excitations that act to confine light into nanoscale dimensions, leading to significant interest in their use as nanoscale optical elements, such as in data carrying device interconnects, polarization manipulators, optical antennas for efficient far field light coupling, routers, modulators, multiplexers, and logic gates [1,3,4]. To truly evaluate the efficacy of nano-optical elements in subwavelength photonic circuits, nanometer spatial resolution is needed to characterize such structures and to understand the influence of bends and kinks in nanowires on surface plasmon propagation. Optical studies have confirmed the propagation of surface plasmons in nanowires by illuminating one end with a laser and measuring light emission from the opposite end of the wire and from sharp bends and kinks [5]. However, optical techniques lack the spatial resolution to image plasmon excitations at the nanometer length scale of relevance in a plasmonic circuit design. Here, utilizing recent advances in electron energy loss spectroscopy (EELS) [6], we find that surface plasmon propagation in silver nanowires is largely unaffected by the presence of sharp kinks and corners, as indicated by direct imaging of multimodal Fabry-Perot-type plasmonic resonances set up in a variety of structures. Further measurements show that the plasmonic field extends to 40 nm normal to the surface of the nanowire at the 1.55 μm wavelength, placing a physical limit on achievable photonic circuit compactness. The analysis is achieved with technological advances in electron microscopy, enabling the detection of low-energy excitations in nanostructures in the midinfrared regime, down to 0.17 eV, with nanometer spatial resolution, an advance that opens up what is widely recognized as an unexplored field [7].

Individual noble metal nanoparticles and nanowires strongly interact with light because of the excitation of collective electron oscillations at the surface of the particle [8]. Electromagnetic waves set up by these charge fluctuations, known as surface plasmon polaritons (SPPs), are bound to the surface of the metal and can propagate nonradiatively along a metallic surface with a broad spectrum of frequencies. This property has led to their central role in the miniaturization of nanophotonic devices [9]. However, the analysis of plasmonic excitations in nanophotonic elements has thus far been limited because of the demanding requirements necessary for the probing technique. Novel scattering-type near-field optical microscopy probes have reached spatial resolutions approaching tens of nanometers in the visible regime [10]; however, near-field microscopy techniques typically suffer from low signal and are limited in long wavelength detection, and it is unclear how the near-field component of the scanning tip potentially affects the electromagnetic local density of states (EMLDOS) of the analyzed material. Alternatively, recent advances in electron microscopy, electron monochromators, and EELS now combine subnanometer spatial resolution analysis with millielectron-volt spectral resolution [11–13], enabling detection in the infrared regime below 1 eV [14,15]. EELS has been used previously to image plasmonic resonances in individual metallic nanoparticles [16–19] and in more exotic structures such as split-ring resonators [20]; however, EELS studies of extended structures with kink and defects, suitable for information transport in nanophotonic devices and not resolved with optical methods, are needed.

We acquired EELS signals from three silver nanowire structures of varying lengths and shapes using a FEI Titan 80-300, equipped with a monochromator and a high-resolution spectrometer operated at 80 keV incident energy extending the approach described previously [14]. The

energy loss spectra were recorded at a resolution of 67 meV (FWHM) with a focused, scanning electron beam approximately 2 nm in diameter. To check our experimental findings, we simulated the electromagnetic response of equivalent nanowire structures using the MNPBEM toolbox [21], which solves Maxwell's equations for arbitrary geometries using the boundary element method.

Figure 1 displays the EELS signals collected from boxed regions enclosing three individual nanowires of approximately the same diameter but different geometry. The first wire is straight and 1215 nm in length, the second wire contains a near 90° bend and is 1034 nm in length, and the third wire contains multiple bends of varying angles and is 2070 nm in length. The nanowires are excited by the transient field of the fast electron [22], and the energy loss is recorded with an EELS spectrometer as discussed in Ref. [23]. The wires support multiple plasmon types with corresponding induced charge oscillations either parallel (longitudinal) or perpendicular (transverse) to the rod axis [24]. The multiple peaks in the spectra below 2 eV are longitudinal type resonances, extending to significantly lower energy (in mid-IR) than our previous work [14]. Between 3 and 4 eV, the EELS signal obtained from a point at the tip of the straight wire (Fig. 1, inset) displays two peaks in the UV region, which we assign to a transverse surface plasmon and a bulk plasmon at 3.42 and

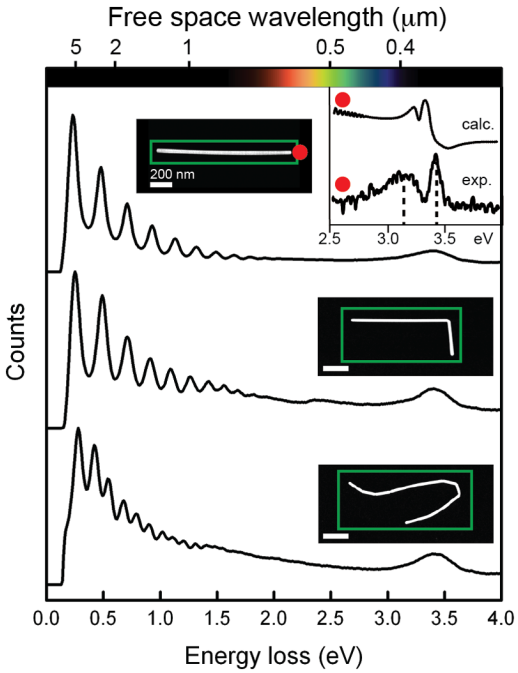

FIG. 1 (color online). The total EELS spectra from the green boxed regions enclosing three different nanowires. The EELS signal recorded at the tip of the straight nanowire (red dot) exhibits two peaks belonging to transverse surface and bulk oscillating plasmons at 3.42 and 3.74 eV, respectively (inset), which are well reproduced by simulation.

3.74 eV, respectively. These modes, present in all the nanowires and confirmed by calculations, are nonpropagating and are of the same type that occurs in spherical nanoparticles.

The energy filtered maps (Fig. 2) display the spatial origin of inelastic electron scattering events at energy transfers belonging to peak positions in the EELS signal. The intensity variation in the maps is representative of the electron energy loss probability, given by the EMLDOS [25]. Similar to previous work on short wires [14], we observe a simple standing wave pattern in the LDOS, set up by the interference of counterpropagating SPPs traveling back and forth along the length of the nanowire. However, with the improved resolution and increased length of the wires, we spatially resolve ten mode orders in each nanowire down to 0.17 eV in energy, significantly lower in energy than previously reported. Interestingly, the distribution of resonant SPP antinode maxima appears unaffected by sharp corners in the bent nanowires for all the excited modes, where the antinode maxima positions are uniformly distributed along their length, akin to the straight wire.

The energy filtered EELS images provide a convenient way in which to measure the dispersion of the surface plasmon in the nanowire. For a given resonance mode, the SPP has an energy, E (the energy loss of the incident electron), and wave number, k, extracted by the measurement of the distance between local intensity maxima in the EELS maps. In contrast to the near-field optical intensity of the SPP standing wave, which has two measured intensity maxima per SPP wavelength, in the case of EELS, the position of the electron that excites the mode also plays a role, leading to four measured intensity maxima per SPP wavelength. That is, for EELS, $k = \pi/(2d_{\mathrm{EELS}})$, where d_{EELS} is the distance between intensity maxima. This relationship provides excellent agreement between the experimental measurements of E and k and the calculated dispersion (E vs k) of an infinite silver cylinder of similar diameter, derived elsewhere [26]. The dispersion data from the three nanowires, plus an additional two straight wires, are plotted against the dispersion of light in vacuum and the calculated dispersion of an infinite silver cylinder (Fig. 3). These long wavelength SPP modes typically exhibit low propagation loss, low field confinements, and high group velocity, making them excellent candidates for waveguide applications. At low k, the speed of the SPP (which add to form the standing wave pattern), determined by the slope of the dispersion curve, approaches the speed of light, but the curve lies to the right of the light line, and therefore the SPP is nonradiative even for nanowires with sharp bends and kinks.

The field associated with a SPP is known to decay exponentially with the distance in the direction perpendicular to the supporting metal-dielectric interface. This field is said to be evanescent as a consequence of the

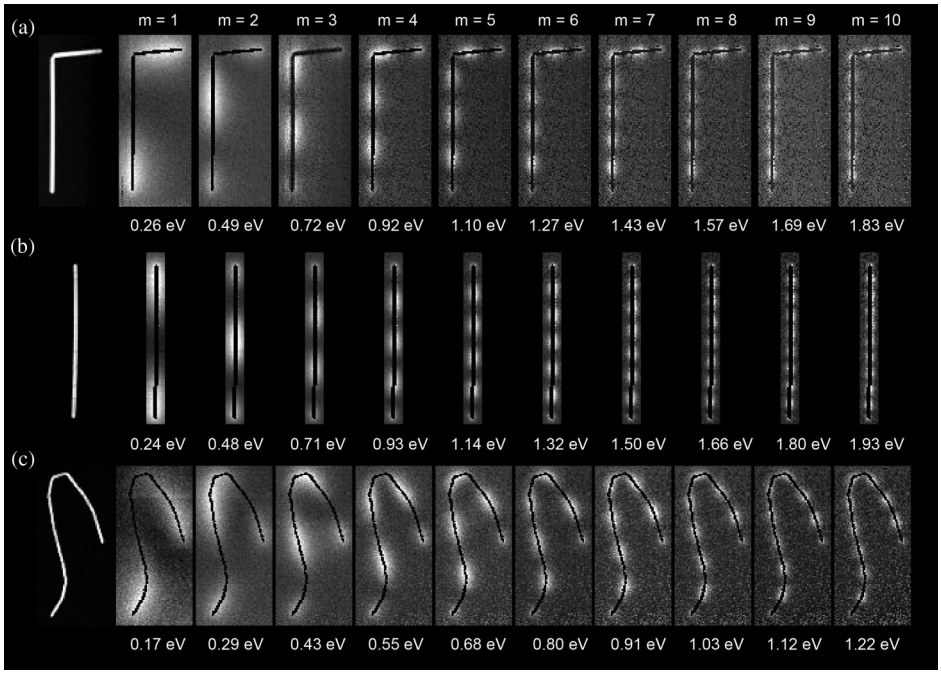

FIG. 2. The variation in EELS signals for nanowires of different shapes at specific energy losses. Three silver nanowires, 1034, 1215, and 2070 nm long, labeled (a), (b), and (c), respectively, support counterpropagating SPPs resonating in the infrared and visible parts of the electromagnetic spectrum.

bound, nonradiative nature of SPPs [27]. A convenient measure of the extent of the evanescent field is the "decay length," which is relevant to the interaction between nanostructures and describes the distance from the surface at which the surface field intensity drops by a factor of $1/e$ into the surrounding dielectric. We thus obtain a measure of the evanescent field decay by recording the intensity of the EELS signal, as a function of both distance perpendicular to the nanowire long axis and of energy loss (Fig. 4). Line profiles, extracted from the EELS projection, display a measure of the evanescent field strength as a function of the perpendicular distance from the nanowire for the various SPP resonant energy losses [Fig. 4(b)]. The data have been fitted with an exponential function of the form e^{-kz}, where z is the distance from the surface, from which the decay length is conveniently calculated. Figure 4(c) displays the measured decay length of each resonant mode order. The experimental measurements are in good agreement with MNPBEM calculations of decay lengths, with the exception of the low order resonances below 0.5 eV, where the calculations underestimate the measured decay lengths. The discrepancy below 0.5 eV may be because of the delocalization of inelastic electron scattering, which varies as a function of energy loss and acts to limit the spatial resolution of inelastic imaging [23]. In the optic fiber telecommunication band between 1.3 and 1.5 μm, the decay length is approximately 40 nm.

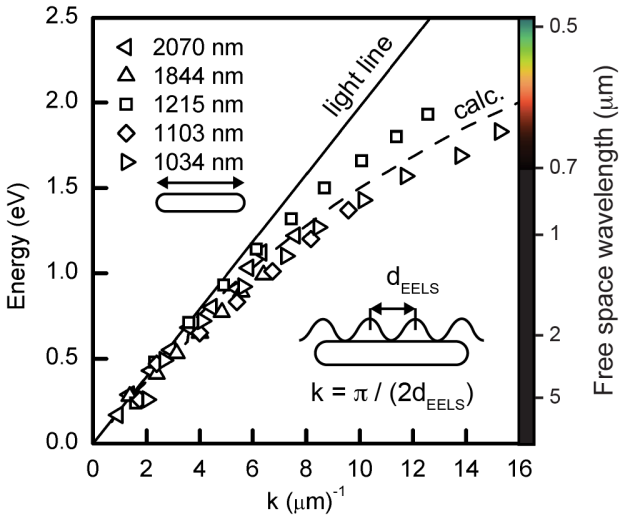

FIG. 3 (color online). The dispersion of resonant SPP waves in silver nanowires of different lengths. The plasmon energy is plotted as a function of the wave number (k). All data are below the light dispersion line in accordance with the SPP classification and are in good agreement with the calculation (dashed line).

Figures 5(a) and 5(b) compare the calculated electron energy loss probability surrounding the bent nanowire at resonance to the experimental EELS maps. We find excellent agreement, and the calculations also show that the modes are unaffected by the near 90° bend in the wire, demonstrating that the sharp kink does not reflect the SPP wave or alter its phase appreciably. This finding is in agreement with the previous work of EELS studies of split ring resonators, where it was found that the basic plasmonic behavior of a split ring resonator was similar to that

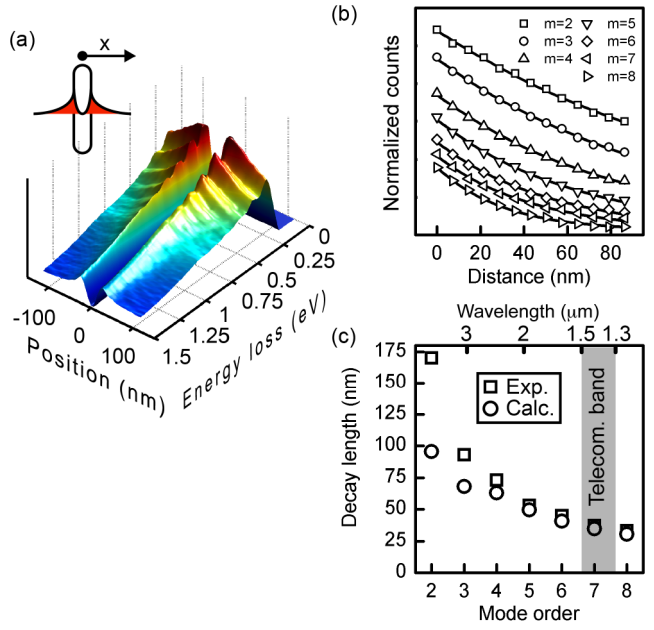

FIG. 4 (color online). Measurement of the exponential decay of the evanescent field from a straight silver nanowire. (a) The SPP LDOS decays exponentially with distance from the nanowire surface and with energy loss as measured by EELS. (b) Line profiles, extracted from the EELS projection in (a). (c) The measured decay lengths of the resonant mode orders (m) are in good agreement with MNPBEM calculations for energies above 0.5 eV. The decay length is approximately 40 nm in the telecommunication band.

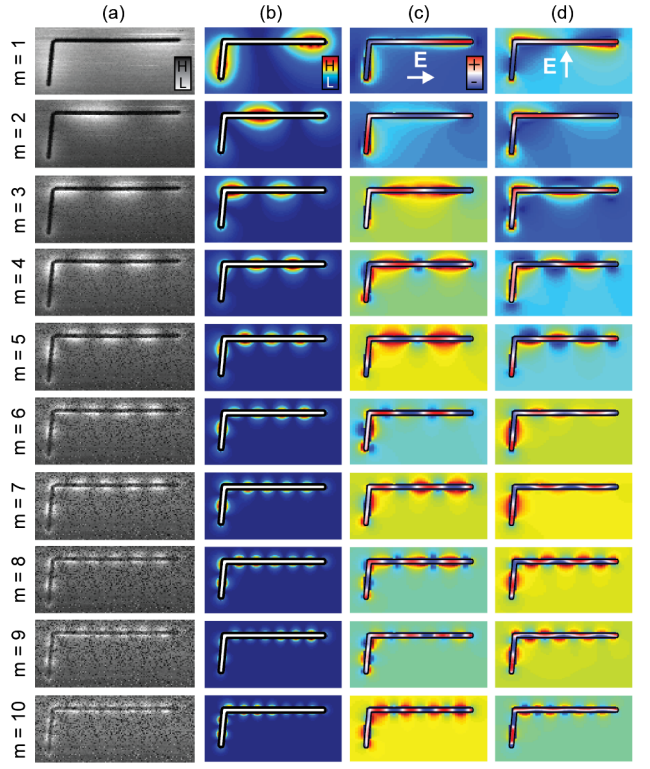

FIG. 5 (color online). The comparison of EELS maps of plasmonic resonances set up in a bent nanowire with calculations for electron and light excitation schemes. (a) Experimental EELS maps of the first ten modes set up in the bent nanowire. (b) Calculated EELS probability maps for a wire structure of the same characteristics. (c) Calculated charge and electric field distributions $|E|^2$ set up on and around the bent nanowire under horizontally and (d) vertically polarized light excitation.

of a nanoantenna of the same cross section [20]. Also, these EELS findings appear to contradict prior observations of photon emission from sharp bends in silver nanowires using simple far-field excitation and detection methods [5,28]. Given that photon emission from the structure would contribute to the electron energy loss process [29], and it is now well established that EELS measurements are closely related to the total EMLDOS [25], our results indicate that there is no light emission from the sharp bends of the nanowire structures. This discrepancy may be because of the presence of discontinuities in the structures studied by light microscopy that were not spatially resolved, which could convert SPPs back to free-space photons detectable in the far field. The simulated response of the bent wire differs significantly when using linearly polarized light instead of electrons to excite the structure. Under both horizontally and vertically polarized light, a distribution of alternating surface charge polarity is set up across the wire, setting up a surrounding electric field [Figs. 5(c) and 5(d)]. It appears that because of the unequal light polarizability of the differently oriented nanowire segments either side of the bend, the local electric field pattern does not exhibit a uniform, strongly bound standing wave distribution across the wire, as in the case of the EELS probability maps. In particular, for the excitation with vertically polarized light a high charge buildup is detected at the corner of the first two modes, suggesting that there are significant differences in the role of the sharp kinks with light excitation as compared to electrons. Based only on these simulations, it appears advantageous to use the electron probe to study the plasmonic properties of such structures. The electron probe can overcome limits on coupling, polarization, and spatial resolution suffered by light-based techniques, resulting in a more interpretable response of structures.

In summary, we have demonstrated the imaging of plasmonic excitations in nanowires, extending into the midinfrared regime by EELS. We have measured SPP dispersion in nanowires of different lengths and found that the resonances are unaffected by sharp bends in the wire. We have also measured the decay lengths of resonant SPP fields, as a function of energy loss, from high-resolution spatial maps. We anticipate that high-resolution full two-dimensional imaging and detection of midinfrared excitations with electrons will impact the study of low energy excitations in a wider range of nanomaterials and photonic nanostructures.

The authors thank F. J. Garcia de Abajo for his analysis of the plasmonic resonances set up in thin wires measured by EELS and valuable discussions, and R. F. Egerton and P. E. Batson for valuable comments on the manuscript. The experimental work was carried out at the Canadian Centre for Electron Microscopy (CCEM), a national facility supported by the NSERC and McMaster University. G. A. B. is grateful to NSERC for a Discovery Grant.

*Corresponding author.
gbotton@mcmaster.ca

[1] V. J. Sorger, R. F. Oulton, R.-M. Ma, and X. Zhang, MRS Bull. **37**, 728 (2012).
[2] S. A. Maier, M. L. Brongersma, P. G. Kik, S. Meltzer, A. A. G. Requicha, and H. A. Atwater, Adv. Mater. **13**, 1501 (2001).
[3] H. Wei, Z. Wang, X. Tian, M. Käll, and H. Xu, Nat. Commun. **2**, 387 (2011).
[4] S. Lal, J. H. Hafner, N. J. Halas, S. Link, and P. Nordlander, Acc. Chem. Res. **45**, 1887 (2012).
[5] A. W. Sanders, D. A. Routenberg, B. J. Wiley, Y. Xia, E. R. Dufresne, and M. A. Reed, Nano Lett. **6**, 1822 (2006).
[6] S. J. Pennycook and C. Colliex, MRS Bull. **37**, 13 (2012).
[7] M. Schnell, P. Alonso-Gonzalez, L. Arzubiaga, F. Casanova, L. E. Hueso, A. Chuvilin, and R. Hillenbrand, Nat. Photonics **5**, 283 (2011).
[8] R. H. Ritchie, Phys. Rev. **106**, 874 (1957).
[9] J. A. Dionne and H. A. Atwater, MRS Bull. **37**, 717 (2012).
[10] M. Schnell, A. Garcia-Etxarri, A. J. Huber, K. Crozier, J. Aizpurua, and R. Hillenbrand, Nat. Photonics **3**, 287 (2009).
[11] M. Haider, S. Uhlemann, E. Schwan, H. Rose, B. Kabius, and K. Urban, Nature (London) **392**, 768 (1998).
[12] P. E. Batson, N. Dellby, and O. L. Krivanek, Nature (London) **418**, 617 (2002).
[13] S. Lazar, G. A. Botton, M.-Y. Wu, F. D. Tichelaar, and H. W. Zandbergen, Ultramicroscopy **96**, 535 (2003).
[14] D. Rossouw, M. Couillard, J. Vickery, E. Kumacheva, and G. A. Botton, Nano Lett. **11**, 1499 (2011).
[15] O. Nicoletti, M. Wubs, N. A. Mortensen, W. Sigle, P. A. van Aken, and P. A. Midgley, Opt. Express **19**, 15371 (2011).
[16] M. Bosman, V. J. Keast, M. Watanabe, A. I. Maaroof, and M. B. Cortie, Nanotechnology **18**, 165505 (2007).
[17] J. Nelayah, M. Kociak, O. Stephan, F. J. Garcia de Abajo, M. Tence, L. Henrard, D. Taverna, I. Pastoriza-Santos, L. M. Liz-Marzan, and C. Colliex, Nat. Phys. **3**, 348 (2007).
[18] M. N'Gom, S. Li, G. Schatz, R. Erni, A. Agarwal, N. Kotov, and T. B. Norris, Phys. Rev. B **80**, 113411 (2009).
[19] B. Schaffer, U. Hohenester, A. Trügler, and F. Hofer, Phys. Rev. B **79**, 041401 (2009).
[20] G. Boudarham, N. Feth, V. Myroshnychenko, S. Linden, F. J. García de Abajo, M. Wegener, and M. Kociak, Phys. Rev. Lett. **105**, 255501 (2010).
[21] U. Hohenester and A. Trügler, Comput. Phys. Commun. **183**, 370 (2012).
[22] F. J. García de Abajo, Rev. Mod. Phys. **82**, 209 (2010).
[23] R. F. Egerton, *Electron Energy-Loss Spectroscopy in the Electron Microscope* (Plenum, New York, 1996), 2nd ed.
[24] M. N'Gom, J. Ringnalda, J. F. Mansfield, A. Agarwal, N. Kotov, N. J. Zaluzec, and T. B. Norris, Nano Lett. **8**, 3200 (2008).
[25] F. J. García de Abajo and M. Kociak, Phys. Rev. Lett. **100**, 106804 (2008).
[26] J. C. Ashley and L. C. Emerson, Surf. Sci. **41**, 615 (1974).
[27] W. L. Barnes, A. Dereux, and T. W. Ebbesen, Nature (London) **424**, 824 (2003).
[28] M. W. Knight, N. K. Grady, R. Bardhan, F. Hao, P. Nordlander, and N. J. Halas, Nano Lett. **7**, 2346 (2007).
[29] N. Yamamoto, K. Araya, and F. J. García de Abajo, Phys. Rev. B **64**, 205419 (2001).